Physicochem. Probl. Miner. Process., 62(3), 2026, 225223

http://www.journalssystem.com/ppmp

Physicochemical Problems of Mineral Processing

ISSN 1643-1049

Optimization of hydrophobic flocculation and magnetic separation of rhodochrosite by sodium oleate

Tingsong Luo [1], Zhenggang Wang [1], Nie Guanghua [1], Qiu TingSheng [2]

[1] Guizhou University School of mining, Guiyang 550025, Guizhou, PRC

[2] Jiangxi University of Science & Technology Jiangxi Univ Sci & Technol, Ganzhou 341000, Jiangxi, PRC

Corresponding author: ghnie@gzu.edu.cn (Nie Guanghua)

Abstract: To address the beneficiation technical challenges in the Guizhou region, where rhodochrosite and quartz are difficult to separate and the recovery rate of fine-grained manganese resources is low, this study conducted experiments using a combined process of sodium oleate hydrophobic flocculation coupled with high-gradient magnetic separation, and systematically elucidated its interfacial action mechanism. The experimental results show that sodium oleate can selectively adsorb on the surface of rhodochrosite particles, forming a dense hydrophobic film, while only weakly adsorbing on the quartz surface, significantly enhancing the differences in surface physicochemical properties between the two minerals. Under the optimal conditions of pH 10, sodium oleate concentration of 4×10^{-5} mol/L, and stirring speed of 600 rpm, selective hydrophobic flocculation of the minerals can be achieved, effectively increasing the particle size of the target mineral, solving the issues of fine manganese loss with quartz and quartz contamination in manganese concentrate. After treatment with high-gradient magnetic separation, the final manganese concentrate grade reached 18.79%, with a manganese recovery rate of 85.84%, an improvement of 8.88 percentage points compared with traditional magnetic separation processes. Combined analyses of zeta potential, contact angle testing, EDLVO theoretical calculations, as well as extended BPMA, FTIR, and XPS characterization confirmed that sodium oleate regulates the surface charge and hydrophobicity of mineral particles through chemical adsorption, effectively promoting the aggregation of manganese-containing mineral particles while maintaining the dispersion state of quartz particles. This study provides important theoretical basis and technical support for the efficient separation and recovery of fine-grained manganese minerals.

Keywords: NaOl, magnetic separation, rhodochrosite, hydrophobic flocculation, quartz

1. Introduction

In rhodochrosite processing systems, manganese carbonate ($MnCO_3$) serves as the primary valuable phase, yet its characteristically fine-grained and brittle texture presents a persistent technical barrier for its upgrading by froth flotation. This is particularly the case in Guizhou Province's deposits, $MnCO_3$ predominantly exists as ultrafine particles (<15 μm) with complex dissemination patterns, significantly complicating beneficiation processes. Both particle size distribution and surface characteristics fundamentally govern mineral floatability, where ultrafine particles (<10μm) typically exhibit reduced collision probability with air bubbles and increased surface hydration effects. This size-dependent behavior necessitates optimized surface modification strategies to enhance hydrophobic interactions during flotation separation (Mackay et al., 2020; Zhu et al., 2020). However, the small mass and large specific surface area of fine particles lead to low collision and adhesion efficiency between particles and bubbles, non-selective adsorption of collectors, high particle solubility, and large dosage of chemicals, resulting in extremely low flotation efficiency(Sivamohan, 1990; George et al., 2004; YIN et al., 2011). Research has demonstrated that at a pH of approximately 10, sodium oleate can selectively flocculate rhodochrosite but not quartz (Zhou, 1996). This enables separation of rhodochrosite from quartz in flotation systems; however, these findings derive predominantly from pure mineral tests. In actual ores,

DOI: 10.37190/ppmp/225223

the presence of other gangue minerals compromises reagent selectivity, making effective separation of rhodochrosite from gangue minerals challenging.

Studies demonstrate that increasing the apparent particle size effectively enhances the magnetic separation recovery of fine-grained minerals (Zhenggang et al., 2023), and increasing the apparent particle size can increase the magnetic force exerted on the particles in the magnetic separator. This can be achieved through several methods, including: shear hydrophobic agglomeration, selective flocculation, oil agglomeration, electrolyte agglomeration and magnetic flocculation (Song et al., 1997; Duzyol et al., 2012; Wu et al., 2015; Han et al., 2016; He et al., 2019; Ding et al., 2023). Zhou et al. investigated hydrophobic agglomeration of rhodochrosite, demonstrating that increased sodium oleate (NaOl) concentrations promote larger aggregate formation with improved morphology (Zou et al., 2021). Sheng et al. investigated hydrophobic agglomeration of rhodochrosite using kerosene and oleic acid, demonstrating that stable aggregates form under specific shear conditions (Shen et al., 2023).

Previous studies have found that the energy barrier between fine particles cannot be overcome to form flocs under lower shear (Boller et al., 1998). Many studies have also shown that the formation and fragmentation of flocs occur at the same time, such that when the shear rate increases, the flocs size decreases (Mpofu et al., 2003).

In summary, the hydrophobic flocculation recovery of rhodochrosite requires further investigation. Notably, few studies have examined flocculation recovery of rhodochrosite ores under controlled chemical regimes and shear fields. NaOl is among the most effective and widely used flotation collector for rhodochrosite. Its molecular structure features double bonds and an 18-carbon hydrocarbon chain, that can induce─hydrophobic flocculation during flotation. Therefore, NaOl is selected as the hydrophobic flocculant of rhodochrosite to increase the apparent size of fine rhodochrosite and realize the magnetic separation recovery of fine rhodochrosite. This study employed sieving analysis, adsorption capacity measurements, contact angle measurements, zeta potential analysis, EDLVO theoretical calculations, molecular simulations, SEM characterization, and other techniques to investigate three critical aspects: (1) fine particle recovery efficiency in magnetic separation, (2) hydrophobic agglomeration behavior, and (3) NaOl-induced aggregate formation under shear forces. The research aims to enhance rhodochrosite recovery while elucidating the underlying agglomeration mechanisms governing fine and ultrafine particle processing in magnetic separation systems.

2. Materials and methods

2.1. Test ore sample

The test samples were obtained from a rhodochrosite mine in Qianbei, Guizhou Province, China. The ores in this area contain mainly rhodochrosite, calcite, dolomite, magnesite, quartz, clay minerals with minor amounts of other minerals. Rhodochrosite is distributed in the ore in strips of fine micrite. Isomorphic substitution of Mn by Ca, and Mg within the crystal lattice renders rhodochrosite exceptionally difficult to liberate (Jiawei et al., 2019). Therefore, this study utilizes representative rhodochrosite ore as the magnetic separation material. The sample was prepared through sequential sampling, crushing, and homogenization. Fig. 1 presents the X-ray diffraction pattern of the prepared sample. The pure quartz mineral was selected from Zhengzhou, Henan Province, China. with a purity of 98.4% SiO_2. Quartz test samples below 74 μm were obtained by hand selection, crushing, grinding and screening, and X-ray diffraction (XRD) analysis was carried out. The analysis results are shown in Fig. 1(b). The pure mineral of rhodochrosite is obtained from the concentrate of a rhodochrosite in Qianbei, Guizhou Province, China after hand selection, crushing, grinding and magnetic separation. The manganese content is above 18% and the particle size is below 74 μm. The artificially blended minerals sample was obtained by mixing the ratio of rhodochrosite to quartz at a weight ratio of 1.

2.2. Test methods

2.2.1. Magnetic separation tests

Rhodochrosite is a weakly magnetic mineral with a specific magnetic susceptibility ranging from (0.126~0.75) × 10^{-6} m^3/kg. Therefore, for the magnetic separation test, the SLon-100 high-gradient pulsed magnetic separator was selected, with a magnetic field strength of 1.2 T. The test procedures

included weighing 100 g of ore sample, adding water to a pulp volume of 1 L, stirring the pulp for 1min, followed by pH adjustment using sodium carbonate and the addition of NaOl. The pulp was then stirred for 10 min with a target shear force. The particle size of the ore sample is 80% -74 μm. The conditioned sample slurry was then treated by the magnetic separator. For this test, the flushing water for the magnetic separator was adjusted, and the pulse stroke time was set to 200 revolutions per minute. With a pulse stroke of 6 min, the electromagnetic vibration was activated and the slurry was introduced to the separator's feed port to start the magnetic separation test. The magnetic concentrates and tailings were dried, weighed, and sampled, and to analyze their grades.

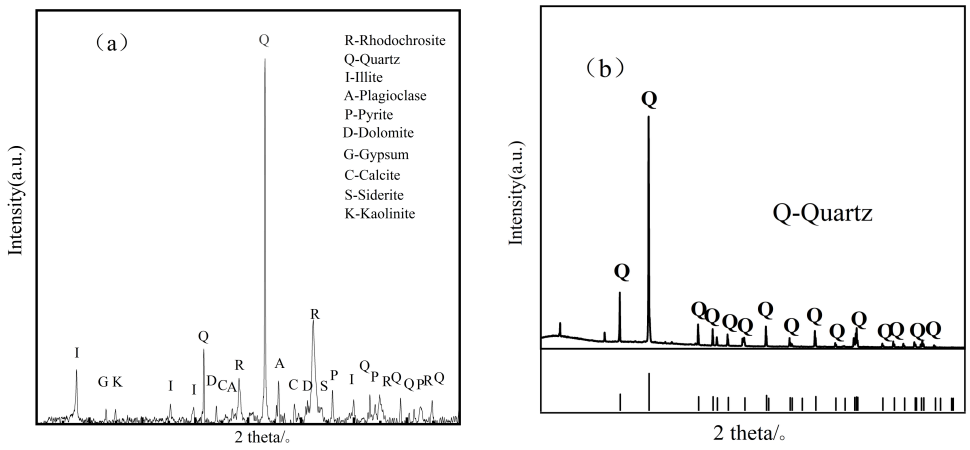

Fig. 1. X-ray diffraction (XRD) diagram (a - rhodochrosite actual ore, b - quartz pure mineral) (the extra bottom pattern on the right figure is the raw ore spectrum)

2.2.2. Contact angle measurements

The contact angle of pure minerals was measured using the JY-82C contact Angle measuring instrument. For each test, 10 g of rhodochrosite and 10 g of quartz were separately weighed and transferred to 200 mL beakers. After adding 100 mL of distilled water to each beaker, the suspensions were agitated for 1 minute. Sodium carbonate pH modifier was then introduced, followed by another minute of conditioning. Then, NaOl was added and the mixture was subjected to 10 minutes of shear conditioning using a JJ-1 electric stirrer, with a rotational speed of 600 rpm. The samples were allowed to settle, filtered and air-dried, and pressed into circular discs using the YP-2 tablet press. Contact angles were measured using a goniometer, with three replicate measurements per sample. Reported values represent the arithmetic mean of these measurements.

2.2.3. Zeta potential measurements

The pure mineral samples were ground to -45 μm and then tested using the DelsaNano C zeta potential analyzer. For each mineral, ten 2 g aliquots were prepared by transferring into 50 mL beakers containing 20 mL distilled water. After 1 minute of agitation, sodium carbonate pH modifier was added, followed by another minute of conditioning. NaOl was then introduced, with subsequent shear conditioning for 10 minutes. Zeta potential measurements were conducted at 25°C using standardized instrument settings. Each sample underwent triplicate measurements, with reported values representing the arithmetic mean.

2.2.4. Theoretical calculation of interaction energy between particles

The interaction energy between quartz is as in Equation 1, the interaction energy between rhodochrosite is as in Equation 2, and the interaction energy between quartz and rhodochrosite is as in Equation 3 (Zhenggang et al., 2023).

$$V_T^{ED} = -\frac{AR}{12H} + 2\pi\varepsilon_0\varepsilon_T R\varphi_0^2 \ln\left[1 + exp(-\kappa H) - 2.51\times10^{-3} R k_1 h_0 exp\left(-\frac{H}{h}\right)\right] \quad (1)$$

$$V_T^{ED} = -\frac{AR}{12H} + 2\pi\varepsilon_0\varepsilon_T R\varphi_0^2 ln[1 + exp(-\kappa H) - 2.51\times10^{-3} R k_1 h_0 exp(-\frac{H}{h}) - \frac{32\pi^2 R^6 \chi^2 B^2}{9\mu_0 H^3} \quad (2)$$

$$V_T^{ED} = -\frac{A_{123}R_1R_2}{6H(R_1+R_2)} + \pi\varepsilon R(\varphi_1^2+\varphi_2^2)(\frac{2\varphi_1\varphi_2}{\varphi_1^2+\varphi_2^2}p+q) - 2.51\times10^{-3}k_1h_0exp(-\frac{H}{h})(\frac{2R_1R_2}{R_1+R_2}) \quad (3)$$

where $A-$ Hamaker constant of mineral particles, (J), $R-$ particle size of minerals (nm), $H-$the distance between the two particles (nm), ε_0- vacuum dielectric constant, 8.854×10^{-12} (F/m), $\varepsilon_T-$the relative dielectric constant of water, φ_0-surface charge of mineral particles, $\kappa-$ Debye length, ($\kappa_{rhodochrosite} = 0.49nm^{-1}$, $\kappa_{quartz} = 0.104nm^{-1}$), k_1- incomplete hydrophobicity coefficient, h_0-attenuation length (nm).

2.2.5. BGRIMM process mineralogy analyzer (BPMA) analysis

Rhodochrosite magnetic separation concentrates, both untreated and NaOl-treated, were air-dried and embedded in epoxy resin to form consolidated specimens. The mounted samples underwent sequential preparation stages: rough grinding, fine grinding, polishing, ultrasonic cleaning in alcohol, and gold sputter coating prior to SEM characterization.

2.2.6. FTIR analysis

The purified mineral sample was further ground in an agate mortar to achieve a particle size of 5 μm. Subsequently, 20 mL distilled water was added and conditioned for 1 minute. Sodium carbonate pH modifier was introduced, followed by another minute of conditioning. NaOl was then added, with shear conditioning applied for 10 minutes. The sample was vacuum-filtered, thoroughly rinsed with distilled water, and dried in a vacuum oven at 40°C for 24 hours. For FTIR analysis, the dried sample was homogenized with potassium bromide (1:100 mass ratio) and pressed into pellets. Spectra were recorded at 25°C using a Nicolet iS20 FTIR spectrometer (Thermo Fisher Scientific, USA) across the 400-4000 cm^{-1} range.

2.2.7. XPS analysis

The prepared pure mineral sample was further ground in agate mortar to less than 20 μm for 5 min. Two (2) g of rhodochrosite and quartz were cleaned by ultrasonic wave and added to 40 mL beaker, followed by the addition of 20 mL of distilled water, sodium carbonate pH adjustment and NaOl addition. The slurry was conditioned for 10 min, filtered, and the filtered solid sample was placed in a vacuum drying oven for 24 hours. X-ray photoelectron spectroscopic measurements were performed on the dried sample using a Thermo Scientific K-AlPHa (Thermo Fisher Scientific, USA) X-ray photoelectron spectrometer. AlKα (1486.6eV) used in the experiment was the sputtering source. The operating voltage and filament current are 15 kW and 10 mA respectively. The pressure in the analysis chamber is less than 5.0×10^{-10} mbar. The full spectrum scan has a pass energy of 100 eV and a step size of 1 eV, while the fine spectrum scan has a pass energy of 50 eV and a step size of 0.05 eV. The quantization and peak fitting of the spectrum were determined using the thermal science advantage software. The binding energy of C1s (284.8 eV) was used to correct the binding energy of each element.

3. Results and discussion

3.1. Magnetic separation test results and analysis

3.1.1. Experimental investigation of NaOl dosage effects

To evaluate the impact of NaOl concentration on rhodochrosite recovery during magnetic separation, comparative tests were conducted using representative ore samples. The resultant beneficiation efficiencies are presented in Fig. 2.

It can be seen from the results of Fig. 2 that, without adding sodium oleate (i.e., without hydrophobic flocculation), the magnetic concentrate recovered about 77% of the rhodochrosite at a grade of 19% Mn. After using NaOl at a concentration of 4×10^{-5} mol/L, the magnetic separation of rhodochrosite showed excellent recovery performance. Under these conditions, excellent results were achieved with a grade of 18.79% Mn and a recovery of 85.84%. Compared to conventional magnetic separation concentrates without adding NaOl, the manganese grade decreased by 0.2 percentage points, while the recovery rate increased by 8.88 percentage points. When the concentration of NaOl was increased, the manganese

grade and recovery rate of the concentrate were both decreased. In the test sample rhodochrosite is present along with calcite, magnesite and other carbonate gangue minerals. Excessive sodium oleate causes the hetero-aggregation of various minerals, deteriorating the separation efficiency and resulting in a decrease in the grade of the magnetic concentrate.

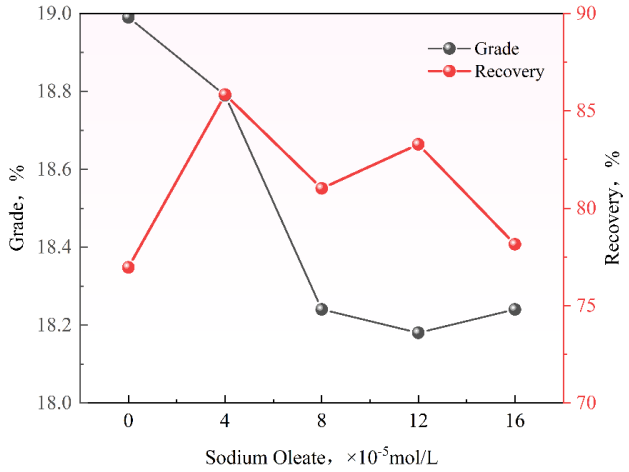

Fig. 2. Experiment on the conditions of hydrophobic flocculation and magnetic separation of sodium oleate, pH 10

3.1.2. Magnetic separation tests at different stirring rate

As shown in Fig. 3, 4×10^{-5} mol/L NaOl was added to the mineral suspension, and the influence of shear force on the magnetic separation of rhodochrosite flocculation was investigated under the condition of pH 10.

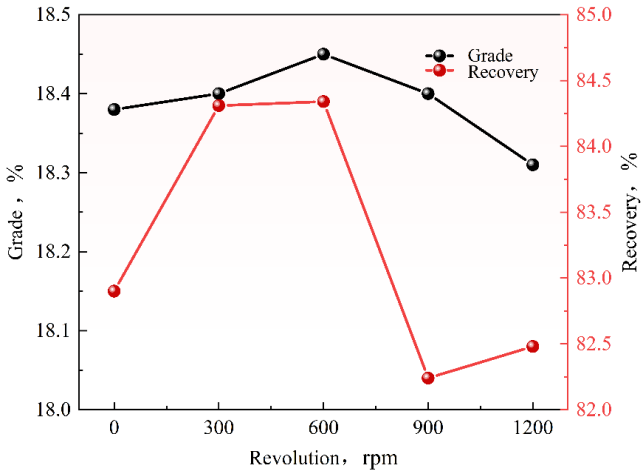

Fig. 3. Stirring rate magnetic separation test

As can be seen from Fig. 3, in five magnetic separation tests with different stirring rates, the images of manganese grade and recovery rate of manganese concentrate showed a peak shape, which is because when the shear rate reaches the critical rate, the rupture rate of aggregates is greater than the formation rate (PARKER et al., 1972; Spicer et al., 1998; Gregory et al., 2001). Too high or too low stirring rate is not conducive to the magnetic separation recovery of manganese carbonate ore. When the stirring rate is 600 rpm, the manganese grade in the concentrate is the highest, and the recovery is also the highest. Similar to previous research results (He et al., 2012; Zhang et al., 2019), the fluid shear force not only affects the formation of aggregates, but also affects their stability. Excessive shear force makes the formed agglomerates easily break back into fine particles, carrying along gangue and fine mud, while also lowering the recovery rate and grade of the magnetic concentrate. Effectively increasing the particle size of rhodochrosite is conducive to its probability of being captured by magnetic medium in magnetic separator.

3.1.3. Study on the particle size of rhodochrosite and quartz in magnetic separation and the flotation effect of sodium oleate

The mineral particle size analysis of conventional magnetic separation and hydrophobic flocculation magnetic separation tailings was carried out. The coarser particle size was analyzed by screening method, and the finer particle size was analyzed by elution method. The analysis results are shown in Fig. 4(a). In order to explore the interaction between the particles of rhodochrosite and quartz during magnetic separation, as well as the effect of adding sodium oleate on the separation of the two minerals. Using the conventional magnetic separation method, under mechanical stirring at 600 rpm, 4×10^{-5} mol/L of sodium oleate was added, the pH was adjusted to 10, and magnetic separation experiments were carried out. The concentrate from the two groups of experiments was sieved and analyzed. The role of sodium oleate in the magnetic separation process was explored. The experimental results are shown in Fig. 4(b).

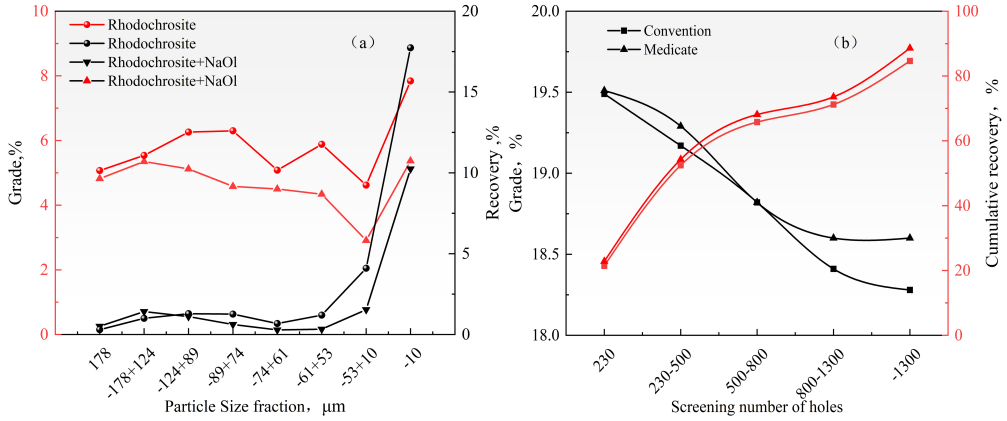

Fig. 4. Screening analysis test before and after NaOA action (a - elution analysis, b - sieve analysis)

From the results in Fig. 4(a), it can be seen that after adding sodium oleate to the rhodochrosite for hydrophobic flocculation, compared with the conventional magnetic separation of each particle size range, the manganese content and distribution rate in the tailings increased as the particle diameter of the mineral decreased. The smaller the particle diameter, the greater the decrease of the grade and distribution rate. It proves that the magnetic recovery of fine particles is beneficial under the action of NaOl, to reduce the probability of gangue mineral fine particles being recovered by magnetic separation. The results of the right Fig. 4(b) show that under the action of NaOl, the grade and distribution rate of fine manganese carbonate in the concentrate increase, and the addition of NaOl is conducive to the magnetic separation of fine manganese carbonate and quartz particles.

3.1.4. Effect of sodium oleate and shear on the settling rate of fine rhodochrosite and quartz

A sedimentation analysis was conducted using rhodochrosite with a particle size of less than 10 μm and quartz. 1 g of the mineral sample was added to each group. One group was also added with sodium oleate at a concentration of 4×10^{-5} mol/L, and the pH of the mineral slurry was adjusted to 10. After applying an external shear force at 600 rpm, measure the turbidity and calculate the sedimentation rate. The test results are shown in Fig. 5.

As shown in Fig. 5, when pH=10, as the standing sedimentation time increases, the turbidity of the supernatant of rhodochrosite and quartz single-mineral suspensions continuously decreases; in the system without reagent, the overall turbidity of the pure quartz suspension is higher than that of rhodochrosite, indicating that fine quartz particles have stronger suspension stability and are more difficult to settle. After adding sodium oleate (NaOl), the supernatant turbidity of both minerals significantly decreases. Sodium oleate can induce hydrophobic aggregation of mineral particles through surface hydrophobic adsorption, accelerating particle sedimentation; moreover, the sedimentation-promoting effect of sodium oleate on rhodochrosite is far better than on quartz, demonstrating that sodium oleate can selectively enhance rhodochrosite aggregation and sedimentation, providing a sedimentation kinetics basis for the efficient flotation separation of rhodochrosite and quartz.

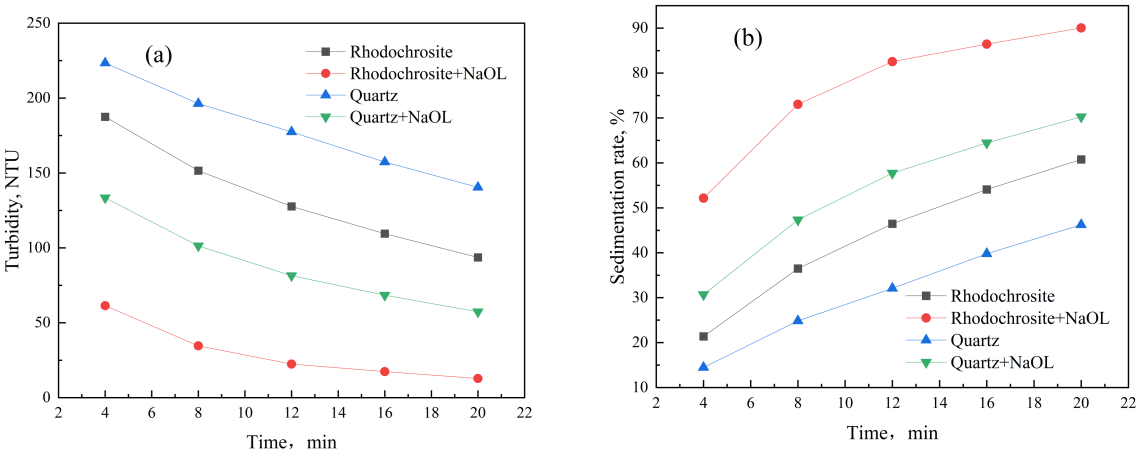

Fig. 5. Settling test of rhodochrosite and quartz before and after NaOl action (a - turbidity, b - sedimentation rate)

3.2. Zeta potential test results

The surface potential of minerals directly determines the electrostatic interaction energy between particles, which in turn regulates particle aggregation and dispersion behavior. So, understanding how the surface potential of minerals evolves is important for revealing the mechanism of particle flocculation and dispersion. Fig. 6 shows the Zeta potential test results of rhodochrosite and quartz single minerals under different pH conditions, before and after treatment with sodium oleate (NaOl). From Fig. 6(a), we can see that the isoelectric point (IEP) of pure rhodochrosite is at pH 8.3. After adding NaOl in a pH 10 system, the Zeta potential of rhodochrosite shifts significantly from -18.8 mV to -45.0 mV, meaning the surface negative charge increases greatly. Fig. 6(b) shows that NaOl has little effect on the Zeta potential of quartz. Interestingly, at pH 10, both minerals carry a large amount of negative charge, with rhodochrosite at -45.0 mV and quartz around -35 mV, creating a strong electrostatic repulsion barrier between the mineral particles. According to DLVO theory, the strength of electrostatic repulsion between particles increases as the absolute value of the Zeta potential goes up.

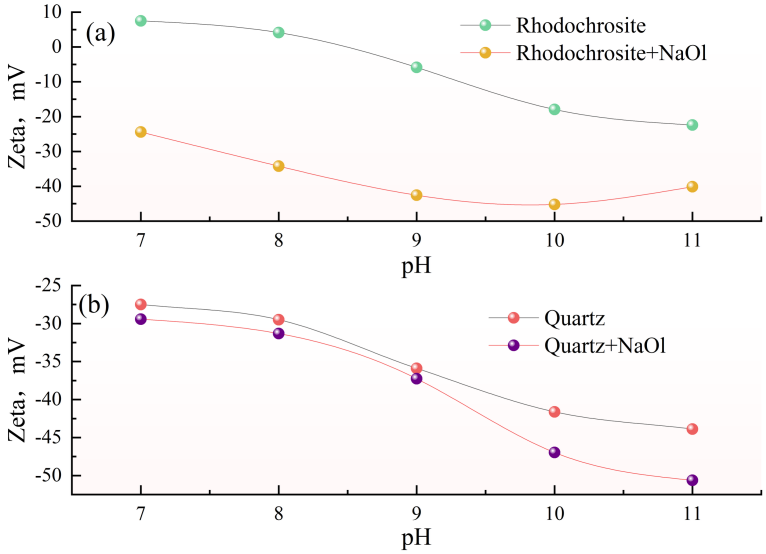

Fig. 6. Zeta potential of rhodochrosite and quartz before and after NaOl action

3.3. Contact angle test results

Particle surface hydrophobicity governs the hydrophobic flocculation of mineral particles. To characterize mineral surface hydrophobicity, contact angle measurements were performed. Fig. 7 presents contact angles for rhodochrosite and quartz before and after reagent treatment. Pretreatment angles measured 52.2°±1° for rhodochrosite (a) and 19.8°±1° for quartz (c), consistent with literature

values. Following pH adjustment and NaOl addition, rhodochrosite (b) exhibited significantly increased hydrophobicity (83.4°±1°) versus minimal change in quartz (21°±1°). This 62° contact angle differential confirms preferential NaOl adsorption on rhodochrosite surfaces. The reagent selectively enhances rhodochrosite's hydrophobicity, promoting shear-induced agglomeration during conditioning. Resultant increases in apparent particle size facilitate magnetic separation recovery through improved capture efficiency.

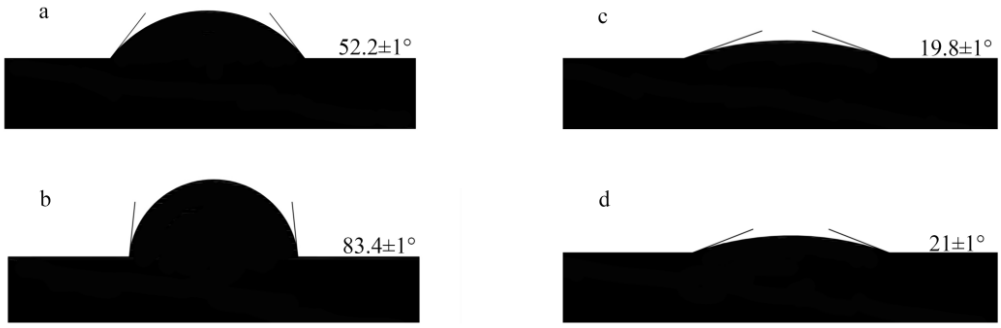

Fig. 7. Contact angle between rhodochrosite and quartz before and after NaOl action ((a) before rhodochrosite action (b) after rhodochrosite action (c) before quartz action (d) after quartz action)

3.4. Interaction energy between particles

Some studies (Zhang et al., 2019) show that particle size and the mineral's specific magnetic susceptibility are the key factors in determining the recovery efficiency of weakly magnetic minerals in high-gradient magnetic separation. The probability of magnetic media capturing the target mineral particles increases with larger particle size and higher specific magnetic susceptibility. Selective flocculation is an effective way to enhance high-gradient magnetic separation performance. This technique can both increase the apparent particle size of the target mineral and prevent hetero-coagulation between the target mineral and gangue minerals, thereby improving the recovery efficiency of magnetic particles. In a pure water system, rhodochrosite and quartz tend to undergo hetero-aggregation. When the aggregates are mainly quartz, the overall specific magnetic susceptibility of the flocs is low, causing the entrapped rhodochrosite to go into the tailings and significantly reducing the recovery of iron concentrate. If the aggregates are mainly carried by limonite, the magnetic properties of the flocs significantly increase, and a large amount of quartz gangue enters the magnetic concentrate, worsening its grade. Calculations of inter-particle forces show that under conditions of slurry pH=10 and sodium oleate (NaOl) dosage of 4×10^{-5} mol/L, the cohesion among rhodochrosite particles is significantly enhanced, increasing the apparent equivalent particle size and effectively improving high-gradient magnetic separation recovery. At the same time, quartz particles remain well dispersed and can efficiently separate from rhodochrosite flocs under the action of the separation water flow. The reagent regulation strengthens the electrostatic repulsion between rhodochrosite and quartz particles, eliminating hetero-aggregation in the original system, increasing the average specific magnetic susceptibility of flocs with the same size, and ultimately achieving efficient magnetic recovery of fine rhodochrosite while reducing tailings loss of fine magnetic minerals.

3.5. BGRIMM process mineralogy analyzer (BPMA) analysis results

As shown in Fig. 9. Using BPMA characterization methods to comparatively analyze the embedding and adhesion characteristics of minerals on the surface of manganese concentrate before and after the action of sodium oleate (NaOl), the results show that: when NaOl is not added, a large amount of quartz and gangue minerals adhere to the surface of the target minerals, and the proportion of clay minerals and fine quartz inclusions inside the ore particles is relatively high, significantly increasing the difficulty of magnetic separation between rhodochrosite and gangue. Ultra-fine quartz particles are often coated on the surface of rhodochrosite in the form of a film. After these composite particles are captured by the magnetic medium, they will directly deteriorate the grade of the magnetic concentrate. At the same time, fine rhodochrosite particles can also be adsorbed onto the surface of quartz particles. If the amount

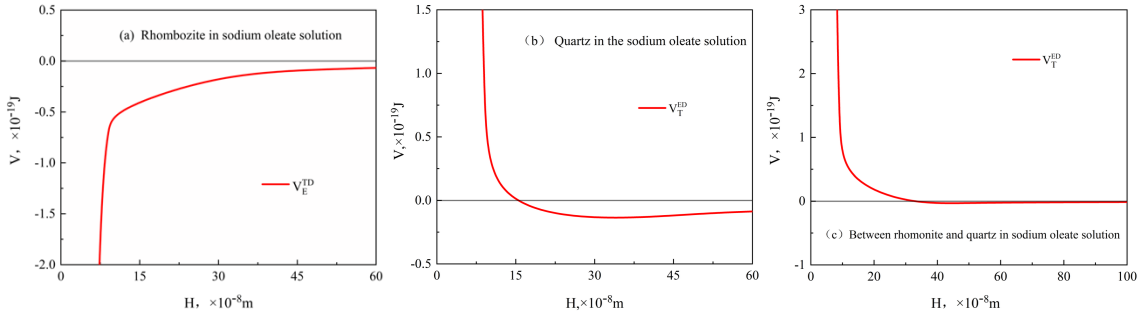

Fig. 8. Interaction energy between rhodochrosite (a) in NaOl solution, quartz (b) in NaOl solution and quartz (c) in NaOl solution

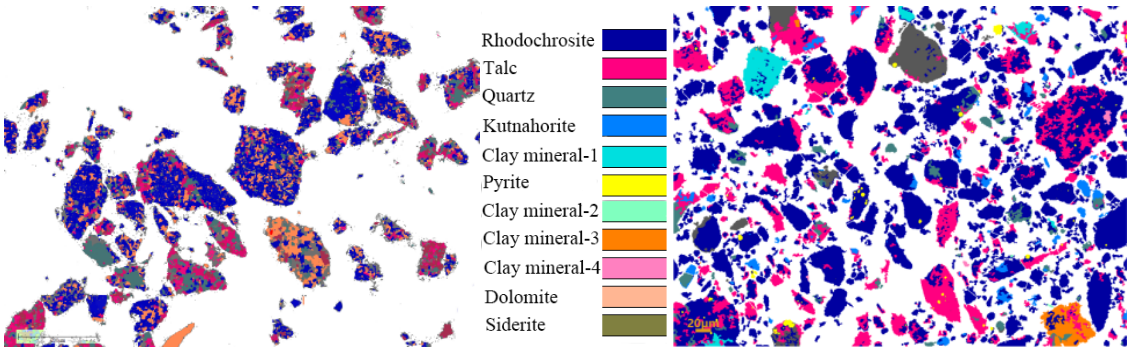

Fig. 9. Analysis of manganese concentrate before and after NaOl action

of rhodochrosite adsorbed on the quartz surface is sufficient, the composite flocs can be recovered by the magnetic medium. However, if the adsorption does not reach saturation, the fine rhodochrosite attached to the quartz surface will be washed away with the sorting water into the tailings, significantly reducing the recovery efficiency of rhodochrosite. After introducing sodium carbonate and NaOl into the slurry system, BPMA images confirmed that the interfacial interaction between quartz and reagents was significantly weakened. The heterogeneous adhesion behavior of quartz attaching to the surface of rhodochrosite and rhodochrosite adhering to the surface of quartz basically disappeared. In the magnetic separation system, only a small amount of individual quartz was covered by a thin layer of rhodochrosite, while most quartz gangue achieved effective dissociation from rhodochrosite. This microscopic adhesion characteristic is highly consistent with the results of the macroscopic magnetic separation tests. Comparing the BPMA observations of the conventional separation system with those of the NaOl-regulated system, it can be seen that the proportion of clay minerals remains high in both systems. This is attributed to the complex mineral composition and highly variable physicochemical properties of the clay minerals, making efficient separation difficult to achieve through reagent regulation, which is an important factor limiting the improvement of separation indices.

According to Fig. 10, the relationship between the dissociation degree of quartz and rhodochrosite and the cumulative recovery rate before and after NaOl action, it can be seen that in the conventional magnetic separation process, quartz mostly has low dissociation degree and forms aggregates with other minerals. After adding NaOl and adjusting the pH of pulp, the quartz particles with low dissociation degree significantly decrease, and the cumulative recovery rate increases linearly. The results show that the agglomerates formed with other minerals are dispersed in the conventional magnetic separation process, and their adsorption on the surface of rhodochrosite is reduced. In the process of conventional magnetic separation, rhodochrosite is mainly composed of low dissociation degree and agglomeration with other minerals. After adding NaOl and adjusting pulp pH, rhodochrosite particles and rhodochrosite agglomeration are mainly composed of high dissociation degree, monomer rhodochrosite particles and rhodochrosite agglomeration, indicating that the agglomeration of rhodochrosite and quartz is dispersed first after adding NaOl and adjusting pulp pH, the new rhodochrosite aggregate is formed between the latter rhodochrosite particles under the action of interparticle force. After NaOl and pH adjustment, the phenomenon of fine rhodochrosite being

absorbed by quartz particles into tailings and fine quartz being absorbed on the surface of rhodochrosite can be effectively reduced, which has a favorable effect on the recovery of rhodochrosite by high gradient magnetic separation.

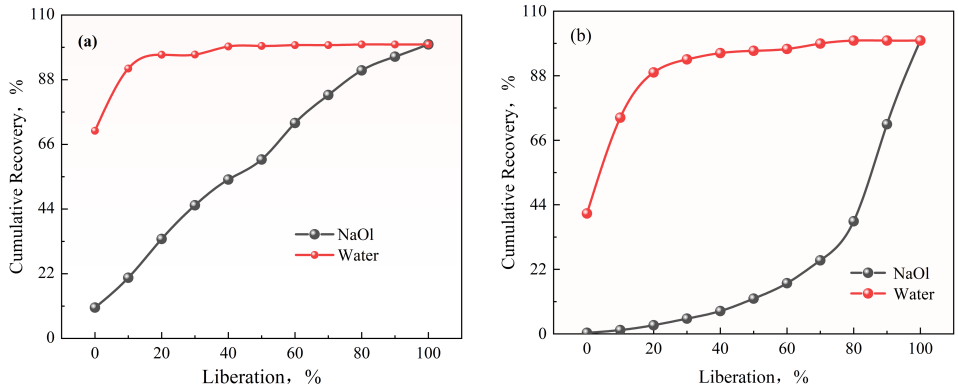

Fig. 10. Dissociation and recovery rates of quartz (a) and rhodochrosite (b) before and after NaOl action

3.6. FTIR analysis

From Fig. 11(a), the infrared spectrum of pure sodium oleate (NaOl) indicates that the absorption peaks at 1562.20 cm^{-1} and 1454.08 cm^{-1} are characteristic peaks of the stretching vibrations of the carboxyl group (-COO^-); the peaks at 2925.00 cm^{-1} and 2852.61 cm^{-1} correspond to the C-H stretching vibrations of methylene (-CH_2) and methyl (-CH_3) groups in the NaOl molecule, respectively. Comparing the infrared spectra of rhodochrosite before and after NaOl treatment in Fig. 11(a), the rhodochrosite samples modified with NaOl exhibit a distinct asymmetric stretching vibration peak of carbonate at 1414.63 cm^{-1}, while bending and stretching vibration bands of carbonate are observed at 864.70 cm^{-1} and 722.97 cm^{-1}; moreover, the characteristic absorption peak of rhodochrosite at 1416.16 cm^{-1} shows a significant increase in intensity, demonstrating that NaOl can stably and extensively adsorb on the rhodochrosite surface. Fig. 11(b) shows the infrared spectra of quartz, indicating that both the peak positions and shapes remain largely unchanged before and after NaOl treatment. In conclusion, NaOl can selectively adsorb on the surface of rhodochrosite and enhance its surface hydrophobicity, which is the intrinsic mechanism underlying the hydrophobic flocculation behavior in the system.

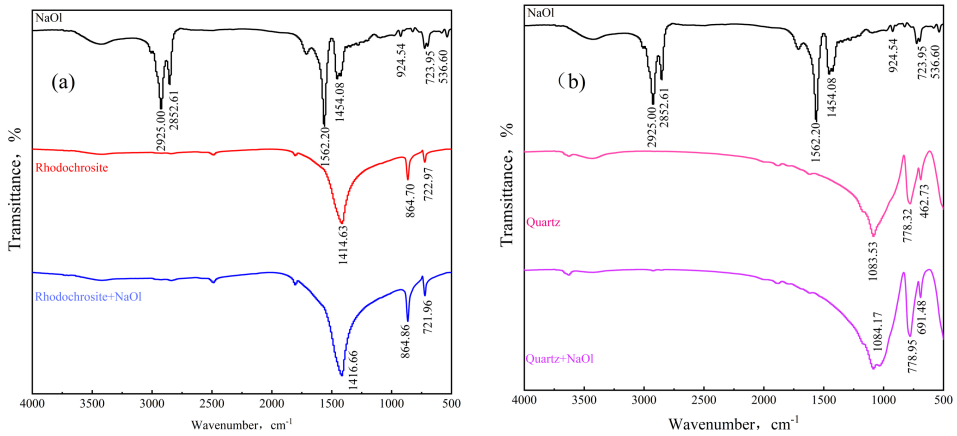

Fig. 11. FTIR diagram of pure minerals (a)-rhodochrosite, (b)-quartz) before and after NaOl treatment

3.6. XPS analysis

The results of XPS full spectrum analysis on the quartz surface are shown in Fig. 12, the fine spectrum of elements on the quartz surface is shown in Fig. 13, and the atomic content of elements on the quartz surface is shown in Table 1.

From the XPS survey spectra of quartz before and after treatment with sodium oleate (NaOl) shown in Fig. 12, it can be observed that no new characteristic diffraction peaks appeared in the quartz samples,

nor were there new element signals in the spectra, indicating that NaOl is unlikely to adsorb on the quartz surface. In contrast, for the rhodochrosite samples, the XPS survey spectra show that after NaOl treatment, a distinct Na1s characteristic peak appears on the sample surface, directly confirming that sodium oleate effectively adsorbs on the rhodochrosite surface.

In order to clarify the changes of elements on the surface of rhodochrosite and quartz after NaOl action, the atomic concentration of each element is listed in Table 1.

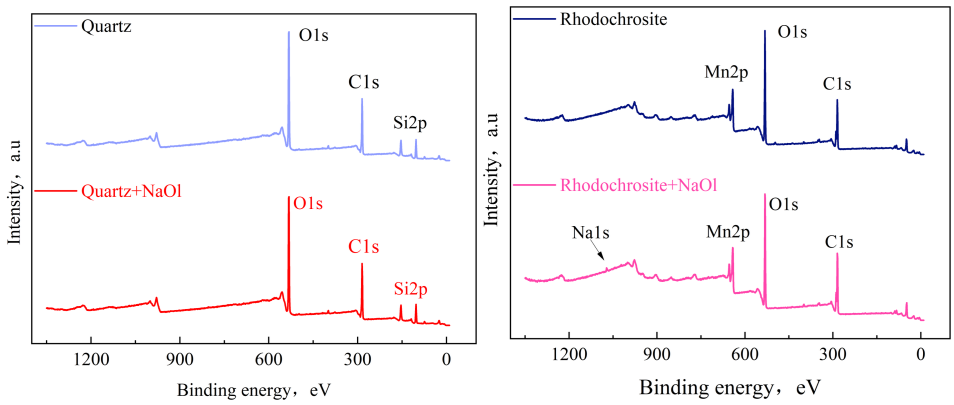

Fig. 12. Full spectrum analysis of quartz and rhodochrosite surface before and after NaOl action

Table 1. Atomic content of surface elements of quartz and rhodochrosite before NaOl action

Sample	Relative content of the major elements, %				
	Si	O	C	Na	Mn
Quartz	14.81	40.67	44.53	0	0
Quartz + NaOl	15.2	39.99	44.8	0	0
Rhodochrosite	0	39.56	53.77	0	7.38
Rhodochrosite + NaOl	0	36.66	55.95	0.89	6.5

According to the test results of the surface element atomic concentration of rhodochrosite in Table 1, it can be seen that after the action of the reagent, the relative content of elements on the mineral surface changed significantly: the atomic concentrations of manganese and oxygen decreased by 0.88% and 2.90%, respectively, the atomic concentration of sodium increased by 0.89%, and the atomic concentration of carbon increased significantly by 2.89%. Among them, the substantial increase in surface carbon content preliminarily confirms that the alkaline reagent can effectively adsorb on the surface of rhodochrosite and form an organic adsorption layer. To further reveal the adsorption mechanism of the reagent on the surface of rhodochrosite, XPS fine peak fitting analysis was performed on the characteristic orbitals C1s, Mn2p, O1s, and Na1s of rhodochrosite before and after reagent treatment, and the specific spectrum results are shown in Fig. 13.

The C1s spectrum of rhodochrosite is dominated by the maximum peak value of 284.78 eV, and two small peaks appear at 289.46 eV and 285.78 eV. After the addition of NaOl, the peak value at 284.78 eV increases significantly, which is attributed to the adsorption of NaOl on the surface of rhodochrosite, resulting in the presence of carbon in NaOl on the surface of rhodochrosite. The results showed that NaOl was adsorbed on the surface of rhodochrosite. The characteristic peaks of Mn2p appear the same in rhodochrosite and rhodochrosite NaOl, and the peaks of Mn2p at 653.88eV become weaker and shift in the direction, and Mn electrons interact with the chemical to form compounds. The characteristic peaks of NaOl in O1s rhodochrosite and rhodochrosite are the same. Na1s did not show a significant peak in rhodochrosite, but showed an obvious characteristic peak at 1071.58 eV after adding NaOl. There were two situations: NaOl adsorbed on the surface of NaOl in molecular form or sodium ion remained on the surface of rhodochrosite. In summary, NaOl can be selectively adsorbed on the surface of quartz and rhodochrosite, changing the surface properties of the two minerals, which is conducive to hydrophobic flocculation of rhodochrosite, increasing the apparent particle size of rhodochrosite,

making rhodochrosite more easily adsorbed on the surface of the magnetic medium in the magnetic separator, and reducing the heterogeneous agglomeration between quartz and rhodochrosite.

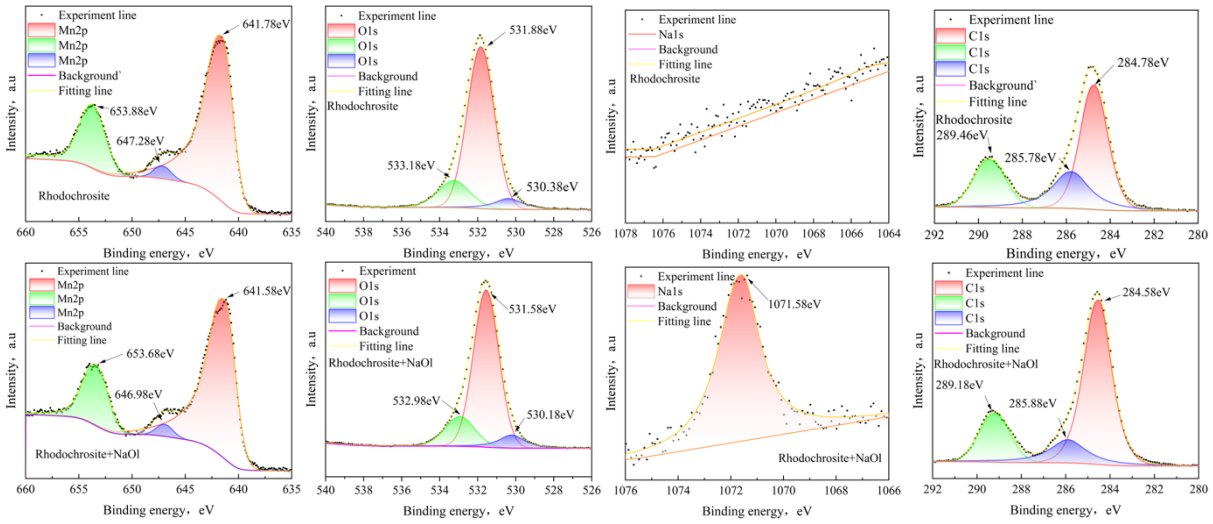

Fig. 13. Fine spectrum of elements on the surface of rhodochrosite before and after NaOl action

4. Conclusions

High-gradient magnetic separation technology can effectively achieve the graded recovery of coarse and fine-grained rhodochrosite, but fine-grained rhodochrosite and quartz particles are prone to hetero-coagulation, which severely interferes with the separation process of fine-grained minerals. The intensity of the pulsed magnetic field is a key parameter affecting the separation efficiency: when the pulse intensity is too high, ultra-fine rhodochrosite particles are easily lost to the tailings with the slurry flow, resulting in a decrease in the recovery rate of the target mineral; when the pulse intensity is too low, fine quartz gangue particles encapsulated or intergrown on the surface of rhodochrosite are difficult to effectively dissociate and remove, ultimately degrading the concentrate grade. By adjusting the slurry pH and introducing sodium oleate, selective flocculation of rhodochrosite can be achieved, effectively suppressing the hetero-agglomeration between rhodochrosite and quartz particles, breaking the agglomeration interference among ultra-fine minerals, and significantly optimizing the separation efficiency of fine-grained rhodochrosite and quartz.

Zeta potential and contact angle test results indicate that under the synergistic regulation of sodium oleate (NaOl) and slurry pH, the physicochemical properties of the rhodochrosite surface change significantly, and the differences in surface characteristics between rhodochrosite and quartz are greatly amplified. NaOl can induce selective flocculation of rhodochrosite particles, forming stable flocs, while quartz particles remain well dispersed; meanwhile, reagent modification significantly enhances the repulsive interaction energy between rhodochrosite and quartz particles, effectively hindering hetero-adsorption and aggregation behaviors between the two mineral particles, providing favorable interfacial conditions for the efficient separation of the two minerals.

BPMA mineralogical analysis results indicate that after adding NaOl, the amount of quartz entrainment in the concentrate is significantly reduced, and the degree of liberation of the target mineral increases linearly, confirming that the hetero-coagulation between rhodochrosite and quartz particles is effectively weakened. Compared with the traditional magnetic separation process, under the reagent-regulated system, rhodochrosite mostly exists as high-liberation individual particles, further proving that the degree of inter-mineral aggregation is greatly reduced. Combined with FTIR infrared spectroscopy and XPS photoelectron spectroscopy test results, it can be seen that NaOl is difficult to adsorb on the quartz surface, can selectively adsorb on the rhodochrosite surface, and modify its surface physicochemical properties, ultimately achieving efficient separation of rhodochrosite and quartz.

In short, by optimizing the sodium oleate (NaOl) reagent scheme and adjusting the slurry pH, we can effectively increase the apparent particle size and floc stability of rhodochrosite, significantly reduce the hetero-coagulation between rhodochrosite and quartz, and make full use of the selective

hydrophobic flocculation properties of the reagent. This helps improve the separation environment both at the interface level and in the particle aggregation structure, ultimately achieving higher high-gradient magnetic separation efficiency and better concentrate quality.

Acknowledgement

Guizhou Provincial Science and Technology Program, Qian Kehe Support [2022] General 225.

References

BOLLER, M. and S. BLASER. 1998. *Particles Under Stress.* Water Science and Technology 37 (10): 9-29.

DING, S., Q. YIN, Q. HE, X. FENG, C. YANG, X. GUI and Y. XING. 2023. *Role of Hydrophobic Fine Particles in Coarse Particle Flotation: An Analysis of Bubble-Particle Attachment and Detachment.* Colloids and Surfaces A: Physicochemical and Engineering Aspects 662: 130980.

DUZYOL, S., A. OZKAN and M. YEKELER. 2012. *Critical Oil–Liquid Interfacial Tension for some Oil-Assisted Fine Particle Processing Methods.* Colloids and Surfaces A: Physicochemical and Engineering Aspects 398: 32-36.

GEORGE, P., A. V. NGUYEN and G. J. JAMESON. 2004. *Assessment of True Flotation and Entrainment in the Flotation of Submicron Particles by Fine Bubbles.* Minerals Engineering 17 (7): 847-853.

GREGORY, J. and V. DUPONT (2001). Properties of Flocs Produced by Water Treatment Coagulants, IWA Publishing.

HAN, H., W. SUN, Y. HU, X. CAO, H. TANG, R. LIU and T. YUE. 2016. *Magnetite Precipitation for Iron Removal From Nickel-Rich Solutions in Hydrometallurgy Process.* Hydrometallurgy 165: 318-322.

HE, W., J. NAN, H. LI and S. LI. 2012. *Characteristic Analysis On Temporal Evolution of Floc Size and Structure in Low-Shear Flow.* Water Research 46 (2): 509-520.

HE, W., Z. XIE, W. LU, M. HUANG and J. MA. 2019. *Comparative Analysis On Floc Growth Behaviors During Ballasted Flocculation by Using Aluminum Sulphate (as) and Polyaluminum Chloride (PACl) as Coagulants.* Separation and Purification Technology 213: 176-185.

JIAWEI, C., L. HUAN, L. XIN and P. ZHIQUAN. 2019. *Process Mineralogy Study of Low-Grade Carbonate Manganese Ore in Xiangxi Region.* Chemical Minerals and Processing 48 (04): 38-41.

MACKAY, I., A. R. VIDELA and P. R. BRITO-PARADA. 2020. *The Link Between Particle Size and Froth Stability - Implications for Reprocessing of Flotation Tailings.* Journal of Cleaner Production 242: 118436.

MPOFU, P., J. ADDAI-MENSAH and J. RALSTON. 2003. *Investigation of the Effect of Polymer Structure Type On Flocculation, Rheology and Dewatering Behaviour of Kaolinite Dispersions.* International Journal of Mineral Processing 71 (1): 247-268.

PARKER, D. S., W. J. KAUFMAN and D. JENKINS. 1972. *Floc Breakup in Turbulent Flocculation Processes.* ASCE J Sanit Eng Div 98 (SA1 Fe): 79-99.

SHEN, Z. and Q. ZHANG. 2023. *Mechanistic Insight of Hydrophobic Agglomeration of Rhodochrosite Fines Co-Enhanced by Oleic-Kerosene Emulsion and Static Magnetic Field.* Separation and Purification Technology 310: 123017.

SIVAMOHAN, R. 1990. *The Problem of Recovering Very Fine Particles in Mineral Processing — a Review.* International Journal of Mineral Processing 28 (3): 247-288.

SONG, S. and O. TRASS. 1997. *Floc Flotation of Prince Coal with Simultaneous Grinding and Hydrophobic Flocculation in a Szego Mill.* Fuel 76 (9): 839-844.

SPICER, P. T., S. E. PRATSINIS, J. RAPER, R. AMAL, G. BUSHELL and G. MEESTERS. 1998. *Effect of Shear Schedule On Particle Size, Density, and Structure During Flocculation in Stirred Tanks.* Powder Technology 97 (1): 26-34.

WU, Y., B. SHI, W. GE, C. J. YAN and X. YANG. 2015. *Magnetic Separation and Magnetic Properties of Low-Grade Manganese Carbonate Ore.* JOM (1989) 67 (2): 361-368.

YIN, W., X. YANG, D. ZHOU, Y. LI and Z. LÜ. 2011. *Shear Hydrophobic Flocculation and Flotation of Ultrafine Anshan Hematite Using Sodium Oleate.* Transactions of Nonferrous Metals Society of China 21 (3): 652-664.

ZHANG, H., L. YANG, X. ZANG, S. CHENG and X. ZHANG. 2019. *Effect of Shear Rate On Floc Characteristics and Concentration Factors for the Harvesting of Chlorella Vulgaris Using Coagulation-Flocculation-Sedimentation.* Science of the Total Environment 688: 811-817.

ZHENGGANG, W., N. GUANGHUA, T. YUN, P. HAISHAN and C. JIANG. 2023. *Study On Condition Prediction and Influencing Factors of Manganese Carbonate Recovery by High Gradient Pulse Magnetic Separation.* Physicochemical Problems of Mineral Processing 59 (3).

ZHOU, L. H. Q. W. 1996. *Study On Hydrophobic Flocculation Flotation of Siderite-Quartz.* Metal Mine(09): 19-22.

ZHU, Z., D. WANG, B. YANG, W. YIN, M. S. ARDAKANI, J. YAO and J. W. DRELICH. 2020. *Effect of Nano-Sized Roughness On the Flotation of Magnesite Particles and Particle-Bubble Interactions.* Minerals engineering 151: 106340.

ZOU, S., S. WANG, H. ZHONG and W. QIN. 2021. *Hydrophobic Agglomeration of Rhodochrosite Fines in Aqueous Suspensions with Sodium Oleate.* Powder Technology 377: 186-193.